Soft Matter

Soft Matter

www.rsc.org/softmatter

ROYAL SOCIETY OF CHEMISTRY

ROYAL SOCIETY OF CHEMISTRY

www.rsc.org/softmatter

Highlight (max. 20 words):

The review addresses the complex interplay between the film surface and core properties on the stability of polylectrolyte/surfactant foam films
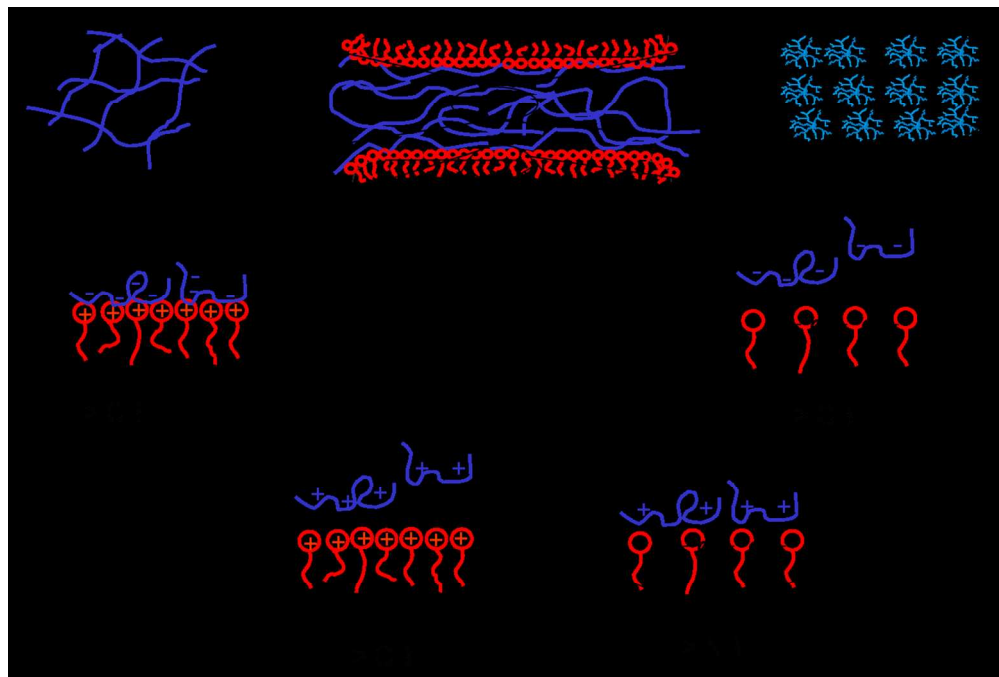
230x154mm (150 x 150 DPI)

ARTICLE TYPE

Effect of polyelectrolytes on (de)stability of liquid foam films

Heiko Fauser and Regine von Klitzing[*a]

The review addresses the influence of polyelectrolytes on the stabilisation of free-standing liquid foam films, which affects the stability of a whole macroscopic foam. Both the composition of the *film surface* and the stratification of the *film bulk* drives the drainage and the interfacial forces within a foam film. Beside synthetic polyelectrolytes also natural polyelectrolytes like cellulose, proteins and DNA are considered.

Introduction

Polyelectrolyte-surfactant mixtures are essential components of many products such as detergents, paints and shampoos[1]. It is important to understand the interactions of such species both in the bulk and at the surfaces to predict their physicochemical behavior and to optimize their performance. According to the application different strengths of interactions between polyelectrolytes and surfactants are required. For instance for decalcification processes strong attraction between polyelectrolytes and surfactant is necessary in order to remove the polyelectrolyte/calcium complexes. In contrast for cleaning products including a polymer for surface protection attraction between polymers and surfactants has to be avoided. However, the interactions between polyelectrolytes and surfactants are quite manifold and include always hydrophobic interactions. Depending on the system electrostatic interaction or hydrogen bonding can be predominant. The performance of these polymer surfactant systems is often based on the foaming properties.

The stability of a foam depends on the stability of single thin films formed by the *continuous liquid phase*. They separate air bubbles which present the *dispersed phase*. During foaming the dynamics within the foam film, *i.e.* drainage plays a decisive role. This is strongly related to rheological properties of the film surface and the film bulk[2,3]. In the last period of drainage interactions between the opposing surfaces become more and more important. They are summarized by the *disjoining pressure* Π and are mainly affected by the composition of the *film surface* and the structuring of complex fluids in the *film bulk*.

The present review addresses foam films containing polyelectrolytes. Their tendency to adsorb at the film surface is often mediated by additional surfactants (part *a* in fig.1). It is assumed that the adsorption of polyelectrolytes at the film surfaces has a strong effect on the stability of foam films due to increase in the elasticity and the change in charge of the film surface. Of course, depending on the charge combination of surfactant and polyelectrolyte also no interaction or even repulsion can take place leading to a pure surfactant layer at the film surfaces (part *b* in fig.1) The first part of the review deals with the effect of the composition of the *film surfaces* on the stabilisation of foam films. Polyelectrolytes can form a type of transient network above the overlap concentration c* in aqueous solutions which causes stratification of foam films (part *c* in fig.1). This phenomenon is rather related to the properties of the *film bulk* and is described in the second part of the review. Again the surface properties are important since the formation of polymer/surfactant complexes at the film surfaces can affect the velocity of stratification. The stratification hamper the drainage and affects the stability of the foam films.
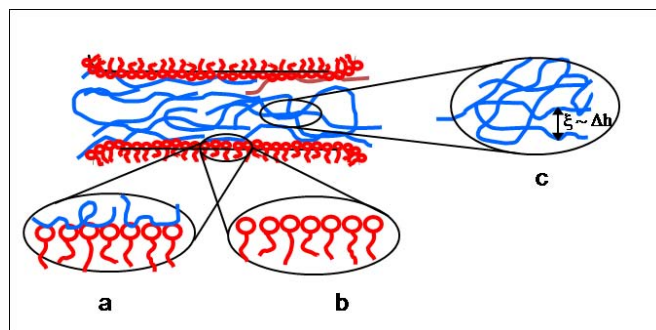
Fig. 1 Scheme of a the structure of free–standing polymer/surfactant foam film a) with strong attraction between polyelectolyte and surfactant leading to surfacae aggregates, b) with no interaction or even repulsion between both compounds and c) formation of a transient polymer network. The mesh size ξ of the network in the film bulk is related to stratification steps Δh

a Stranski-Laboratorium für Physikalische und Theoretische Chemie, Institut fr Chemie, Technische Universitt Berlin, Strasse des 17.Juni 124, D-10623 Berlin, Fax: +49-30-3142-6602; Tel: +49-30- 3142-3476; E-mail: klitzing@chem.tu-berlin.de

1   Methods

The disjoining pressure is an excess pressure within the thin film with respect to the pressure of the liquid in the meniscus. It can be measured with a Thin Film Pressure Balance (TFPB) in dependence of the film thickness h resulting in a disjoining pressure isotherm $\Pi(h)$. The TFPB with porous plate technique was developed by Mysels[4] and Exerowa[5,6]. It is mainly used to study foam films, but recently it has been also extended to study wetting films[7,8]. Thereby the foam film is formed over a 1 to 2 mm hole that is drilled into a porous glass plate. It is enclosed within a pressure–controlled cell and connected to the outer atmospheric pressure. The film thickness is measured interferometrically. More detailed information about TFPB and interaction in foam films are given in former reviews[7,9,10].

By increasing the pressure within the cell against the atmospheric pressure the film starts to drain until repulsive interactions (positive disjoining pressure) between the opposing surfaces prevents further thinning. In mechanical equilibrium the disjoining pressure compensates the capillary pressure. Typical repulsive interactions are electrostatic or steric ones, the main attractive contributions are based on van der Waals forces. Structuring of mesoscopic objects like micelles or macromolecules leads to oscillatory disjoining pressure curves. The mesoscopic object are expelled layer–wise form the film which causes alternating attraction (depletion forces) and repulsion, i.e. oscillatory force. Due to the fact that the TFPB measures only the repulsive parts of the force oscillation, only jumps in film thickness are detected. This step–like thinning is called *stratification* of the foam films.

Another method to study the structuring of complex fluids under confinement is a Colloidal Probe–AFM (CP–AFM)[11]. Instead of a tip, a several micrometer large Silica sphere (colloidal probe) is glued at a cantilever and the force is measured between the sphere and a planar Silicon wafer through the complex fluid. In contrast to a TFPB a CP–AFM allows measuring the full oscillation between two solid surfaces if the soft cantilever are used. Therefore CP–AFM is preferred to TFPB for studies of the structuring of complex fluids under confinement in thin liquid films. Nevertheless, a TFPB can be better used to quantify the non-equilibrium dynamics/drainage between fluid surfaces. Fig. 2 presents a scheme of the free–standing film in in a TFPB and of a film between two solid surfaces in a CP–AFM.

2   Influence of surface composition on foam film stability

Most of the polyelectrolytes in water do not form stable foam films due to a missing amphiphilic character. Surfactants have
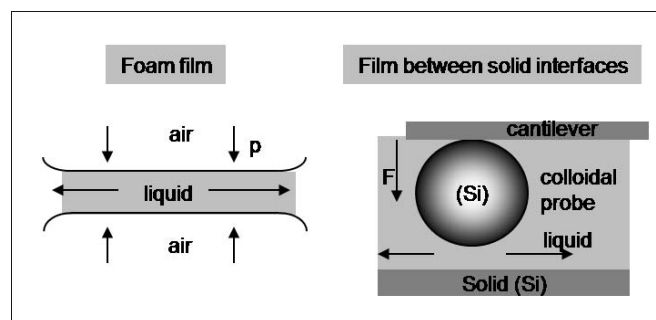

Fig. 2 Scheme of a free–standing film in a Thin Film Pressure Balance (TFPB) (left) and of a film between two solid surfaces in a Colloidal Probe– AFM (CP–AFM)(right).

to be added to form stable films. In this case the interaction between surfactant and polyelectrolyte plays a decisive role on the drainage and stability of foam films and therefore of the macroscopic foam. This chapter addresses the correlation between surface properties and the stability of foam films. The surface properties of aqueous polymer/ surfactant mixtures are mainly determined by tensiometry[12,13]. Other methods are x-ray and neutron reflectometry[14,15] and surface rheology techniques[16,17].

Depending on the charge combination of the used polyelectrolytes and surfactants, either an electrostatically stabilized common black film (CBF) or a sterically (entropically) stabilized Newton black film (NBF) is formed as a final state before film rupture[10].

2.1   Oppositely charged polyelectrolytes and surfactants: Formation of surface aggregates

This chapter addresses aqueous mixtures containing oppositely charged surfactants and polyelectrolytes.

2.1.1   Surface tension   Firstly, a short overview is given about general aspects of the effect of polyelectrolytes on the surface tension. Figure 3 shows a characteristic surface tension isotherm for a mixture of oppositely charged polyelectrolytes and surfactants. Surface tension curves are usually depicted with fixed polyelectrolyte concentration and varied surfactant concentration. A typical concentration range is from 10^{-4} to 10^{-2} (mono)mol/l (polyelectrolyte concentration refers to the concentration of monomer units) for the polyelectrolyte and 10^{-6} to 10^{-1} mol/l for the surfactant. The general features of a surface tension curve of oppositely charged polyelectrolytes and surfactant are well explained in the book of Goddard and Ananthapadmanabhan[19]: Already at low surfactant concentrations, the addition of polyelectrolytes leads to the formation of surface active complexes that lower the surface tension compared to the one of the pure surfactant solu-
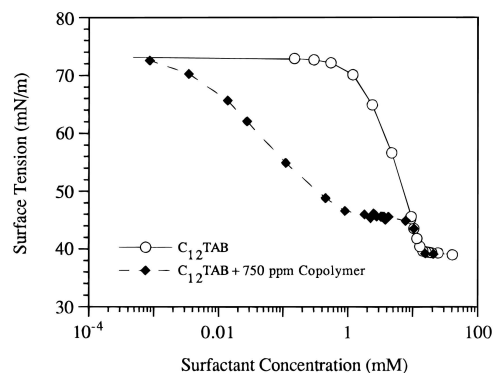
Fig. 3 Surface tension isotherm for a pure cationic surfactant versus an oppositely charged surfactant-polyelectrolyte mixture. At the abscissa the surfactant concentration. "PAMPS25" refers to 25 % charged PAMPS. The PAMPS25 concentration of 750 ppm corresponds to a concentration of $3.5 \cdot 10^{-3}$ (mono)mol/l. The graph is taken from reference [18].

tion. A plateau in surface tension starts close to the critical aggregation concentration in bulk (cac). In this concentration regime, added surfactant is incorporated into bulk aggregates and it does not adsorb at the surface. Related to this the solution is often turbid and no homogeneous foam films can be formed above the cac. Therefore, the concentrations for polyelectrolyte and surfactant should be kept below the cac for quantitative analysis of disjoining pressure isotherms. Upon further addition of surfactant, the surface tension decreases until the critical micelle concentration (cmc) is reached. In this surfactant concentration regime the slope of the surface tension curve is almost the same as for the pure surfactant system which leads to the conclusion that no polymer is adsorbed at the surface anymore. An explanation could be that the surface aggregates become hydrophobic, they desorb and precipitate leading to a pure surfactant surface layer.

So far, the general aspects of the surface tension curves are described. Depending on the specific system, there are several specific features in the surface tension curves in terms of cac, width of the surface tension plateau and cmc [13]. Examples are given in the following.

A strong synergistic lowering of the surface tension is found for mixtures of the cationic surfactant dodecyltrimethyl ammonium bromide (C_{12}TAB) and the anionic polymer poly(acrylamidomethylpropanesulfonate) sodium salt (PAMPS) [12,18] as shown in figures 3 and 4. In presence of PAMPS the surface tension is not affected by the amount of polymer for the concentration range studied. This is explained by polymer stretching at the air/water interface in order to form a neutral complex with the surfactant. Also, the cmc is not affected by the addition of polyelectrolytes.

In contrast to this, for C_{12}TAB / polystyrene sulfonate (PSS) mixtures the plateau region (*i.e.* cac) is very sensitive to the ratio between surfactant and polyelectrolyte concentration and to the absolute concentrations. With increasing polyelectrolyte concentration the surface tension decreases, the region of the plateau becomes broader and the plateau is shifted to higher surfactant concentrations [10]. This is explained by higher surfactant concentration that is required to form hydrophobic bulk complexes at a higher polyelectrolyte concentration.
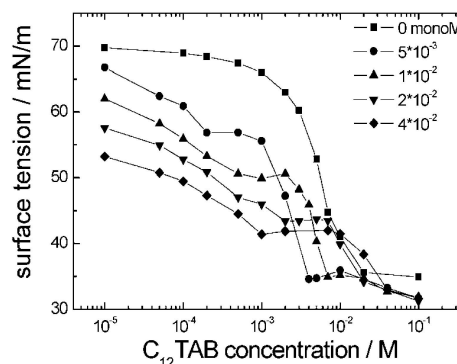

Fig. 4 Surface tension measurements of PSS/C_{12}TAB solutions with different PSS concentrations. The graph is taken from reference [10].

The differences to PAMPS (where no effect of the PAMPS concentration could be detected) is explained by the stronger hydrophobicity and a more bulky molecular structure of PSS in comparison to PAMPS. Hydrophobic effects become even more evident for mixtures with C_{16}TAB: PSS even *increases* the surface tension of the C_{16}TAB solution, since the aliphatic surfactant chain interacts with the hydrophobic PSS backbone. Hydrophilic complexes are formed which reduces the adsorbed amount with respect to pure C_{16}TAB [20].

Beside the polyanion concentration also the polyanion charge affects the plateau in the surface tension. As an example a mixture of the cationic C_{12}TAB and the anionic polysaccharide carboxymethylcellulose (carboxyCM) [21–24] is given. CarboxyMC is a water-soluble random block copolymer derivative of cellulose. It can be obtained from cellulose (consisting of β-D-glucose units) by substituting the hydroxyl-groups with sodium carboxyl. By degree of substitution the charge density can be varied. With increasing degree of charge the plateau is extended over a broader surfactant concentration regime, since more surfactant is needed to hydrophobise the polyanion/surfactant complexes.

In presence of the oppositely charged polyelectrolyte the cmc can be shifted as shown in fig. 4. On the one hand polyelectrolytes can act as a salt which leads to a decrease in cmc

due to electrostatic screening of the surfactant charges. On the other hand the aggregation of polyelectrolytes and surfactants causes a decrease in effective concentration of free surfactant molecules which increases the cmc.

Most of the studies investigate the combination of cationic surfactant and polyanion. The addition of polycations to an anionic surfactant was also studied and show basically the same general features as for the opposite charge combination [7,25].

The different examples for oppositely charged polyelectrolytes and polyanions show that beside general features there are many system specific effects. The most dominant factors affecting the surface tension are the ratio between surfactant and polyelectrolyte concentration, the all overall concentration and molecular parameters like charge density and bulkiness of the polyelectrolyte. Furthermore the hydrophilic/hydrophobic balance of polyelectrolytes and surfactant play an important role since it determines whether electrostatic or hydrophobic interaction dominate the formation of complexes. This in turn decides about the hydrophobicity of the complexes.

2.1.2 Foam films The addition of polyanions (e.g. PAMPPS, PSS) to C_{12}TAB solutions has a strong effect on the foam film stability. Although no foam films can be stabilized from pure C_{12}TAB solutions at concentrations below its critical micellar concentration (cmc: $1.5 \cdot 10^{-2}$ mol/l)[26], the addition of PAMPS or PSS to even low concentrations of C_{12}TAB results in stable foam films [16,27,28]. This stabilization results from the co– adsorption of polymer–surfactant complexes at the interface, which reduces the surface tension. On the other hand, the surface tension itself is not always a measure for the stability. For instance sodium dodecyl sulfonate (SDS) solutions with a surface tension of about 70 mN/m *i.e.* close to the one of pure water can form stable foam films, while C_{12}TAB cannot. This phenomenon hasn't been fully clarified, yet. An important size which decides about foam and foam film stability is the surface elasticity. A high elasticity is assumed to suppress surface undulations and leads to more stable films[29]. So far, most of the surface rheology experiments are carried out for pure surfactant systems and only for one type of surfactant, e.g. C_nTAB[30,31]. As our knowledge a comparison between surface rheology data of different surfactant systems and their impact on foam film stability is still missing. It is even more complex for surface rheology data of polymer/surfactant mixtures. Only a few studies exist (e.g.[16,17,32]) and there is still a lack of understanding the correlation with film stability as shown below.

The stability of foam films is very sensitive to the hydrophilic/hydrophobic balance of the added surfactant. Stable foam films for mixtures beyond $3.8 \cdot 10^{-3}$ (mono)mol/l carboxyMC with 10^{-4} mol/l C_{12}TAB were reported[33]. In case

of C_{14}TAB and C_{16}TAB a significantly lower surfactant concentration of 10^{-5} mol/l was sufficient to obtain stable films. Films made with C_{12}TAB were less stable than those with C_{14} or C_{16}TAB. For all combinations only electrostatically stabilized CBFs were formed. But in all cases stratification occurred. Remarkably, trends exhibited by the stratification kinetics were opposite to the trends in stability. A deeper insight into this phenomena is given in section 3.

2.1.3 Role of the isoelectric point (IEP) In case of C_nTAB/polyanion mixtures a CBF is formed and stable up to moderately high pressures. Since CBFs are stabilized by electrostatic repulsion between the two opposing interfaces, either the surfactant or the polyelectrolyte should determine the sign of surface charge. In order to study the origin of surface charge Kristen et al.[32] measured disjoining pressure isotherms for different combinations of C_{14}TAB and fully charged PAMPS100. In contrast to the more common protocol in which the polymer concentration is fixed and the amount of surfactant is varied, foam films from solutions of a fixed surfactant concentration (10^{-4} mol/l) and variable polyelectrolyte concentration were investigated. Before the studies started the working hypothesis was the following: For concentrations with excess of C_{14}TAB it was assumed that the surface is positively charged, whereas for an excess of PAMPS the surfaces should be negatively charged. When both concentrations are equal the charges should compensate each other what is referred to as the nominal isoelectric point (IEP). At the nominal IEP, where electrostatic repulsion between the opposing film surfaces should be reduced, two scenarios are possible: formation of a NBF or destabilization of the film. The surface charge can be tuned by the variation of the added polyelectrolyte and as a consequence the stability of the foam film may be affected. Figure 5 displays the stability of the foam
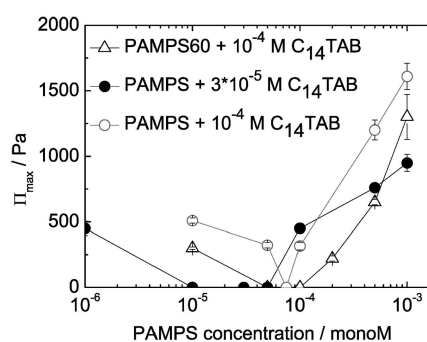

Fig. 5 Stability of PAMPS/C_{14}TAB foam films for systems with different IEP. • IEP = $3 \cdot 10^{-5}$ mol/l ; △ IEP = $1.6 \cdot 10^{-4}$ mol/l; ○ IEP = 10^{-4} mol/l. The graph is taken from reference[17].

films. In this graph the maximum applicable disjoining pressure before film rupture versus the polyelectrolyte concentra-

tion is shown. The nominal IEP for the mixture with 10^{-4} mol/l $C_{14}TAB$ mixture (○) is at 10^{-4} (mono)mol/l PAMPS100. The graph shows that stable films are formed below the IEP. With increasing polyelectrolyte concentration the stability decreases up to a minimum close to the IEP, where no film can be formed. The reason for the fact that the minimum in stability is not exactly at the nominal IEP could be that the surfactant is not completely dissociated or that the surfactant/ polyelectrolyte mixing ratio at the surface is different from that in the bulk. Beyond the IEP the film stability increases again. All films formed were CBF and no NBF formation was observed.

Obviously, the concentration ratio between surfactant and oppositely charged surfactant plays a decisive role. Further studies investigated the influence of the surfactant concentration and the charge degree of the polymer on foam films stabilized by $C_{14}TAB$ and PAMPS [17]. Decreasing the degree of polymer charge results in a shift of the stability minimum to higher polyelectrolyte concentrations as shown in fig.5. A decrease in surfactant concentration leads to a shift in the stability minimum towards lower polyelectrolyte concentrations.

From the stability measurements it seems reasonable that the foam films are stabilized by cationic net charges below and by negative net charges above the IEP due to charge reversal. This would imply a monotonous increase in adsorbed amount of polyanion with increasing polyanion concentration. Additional experiments investigating surface tension and surface dilatational elasticity revealed that this image is much too simple [16,17]: Close to the IEP the amount of adsorbed material seems to be the highest in the measured concentration regime but is decreases towards lower and higher concentrations. Obviously, polymer concentration regimes with high surface coverage but low net charge show low stability, whereas in regions of low surface coverage very stable foam films were observed. This result indicates that the net charge within the foam film plays an important role in foam film stabilization.

It has to be taken into account that the nominal IEP of the systems can deviate from the IEP of the surface. Unfortunately, the IEP of the film surface is difficult to access.

2.2 Mixtures of non–aggregating polyelectrolytes and surfactants

Mixtures of polyelectrolytes with equally charged or nonionic surfactants are supposed to interact weakly with each other. Surprisingly, for both cases stable foam films could be observed [34,35]. Foam films formed from C_nTAB/carboxyMC mixtures are less stable compared to mixtures with the anionic surfactant dioctyl sulfosuccinate (AOT). This leads to the conclusion that the presence surface complexes of surfactants and polyelectrolytes is not the only reason for a stabilisation of foam films of polyelectrolyte/surfactant mixtures.

2.2.1 Equally charged polyelectrolytes and surfactants
Langevin and coworkers intensively studied mixtures of the anionic surfactant AOT with the anionic polyelectrolyte PAMPS25 [18] [12]. Figure 6 and figure 7 show that the addition of PAMPS25 to the equally charged AOT has an almost negligible effect on surface tension, and thickness and stability of the foam film. The surface tension curves show clearly that no
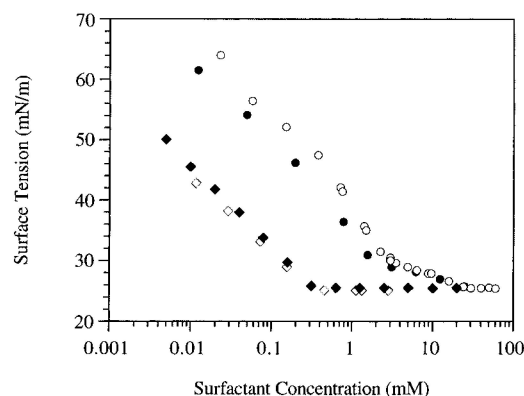

Fig. 6 Effect of PAMPS25 on AOT surface tension isotherm with and without added salt. ○ pure AOT; ● AOT + $3.5 \cdot 10^{-3}$ (mono)mol/l PAMPS25; ◇ AOT + 10^{-1} mol/l NaCl; black diamond: AOT + 10^{-1} m NaCl + $3.5 \cdot 10^{-3}$ (mono)mol/l PAMPS25. The graph is taken from reference [12]

surface complexes of AOT and PAMPS are formed, since the plateau is missing, but that the polyelectrolyte acts rather like a simple salt. The addition of 0.1 M NaCl has a much stronger effect on surface tension and film thickness than the addition of $3.5 \cdot 10^{-3}$ (mono)mol/l PAMPS. The cmc is shifted to lower surfactant concentrations and the foam film becomes thinner due to electrostatic screening.

In all cases the disjoining pressure isotherms reveal CBFs stabilized by an electrostatic double layer.

2.2.2 Equally charged vs. non–ionic surfactants
Mixtures of the cationic polyelectrolyte poly(diallyldimethylammonium chloride) (PDADMAC) with either equally charged cationic surfactant ($C_{16}TAB$) or nonionic surfactant dodecyl-α-maltoside ($C_{12}G_2$) show a completely different stability and disjoining pressure as for thin foam films stabilized by the respective pure surfactants [36–38].

On one hand, the addition of PDADMAC to one of the surfactants has no significant influence on the surface tension isotherms (figure 8). No surface active complexes are formed in both cases.

On the other hand, significant differences in disjoining pressure isotherms are observed. Disjoining pressure isotherms of foam films stabilized by 10^{-4} mol/l of pure $C_{16}TAB$ and by a mixture of 10^{-2} mol/l $C_{16}TAB$ and $5 \cdot 10^{-3}$ (mono)mol/l
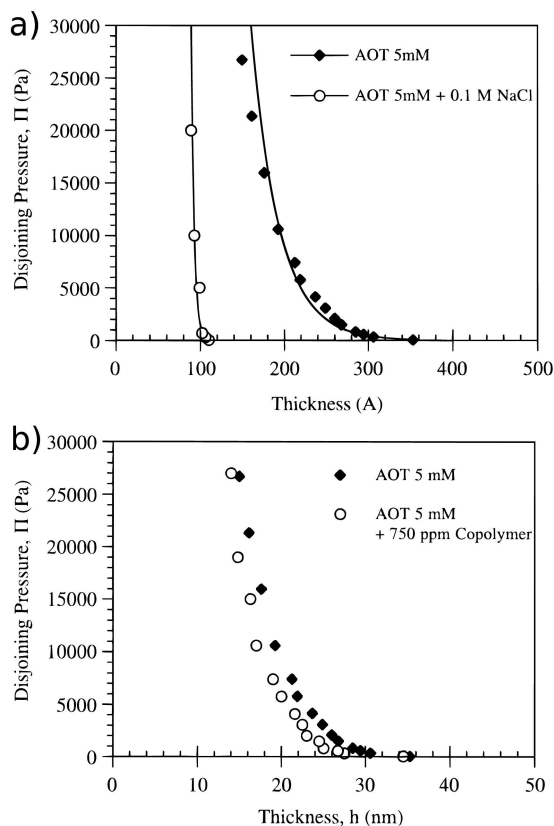
Fig. 7 Disjoining pressure isotherms for a) $5 \cdot 10^{-3}$ mol/l AOT solutions, with and without 10^{-1} mol/l NaCl added, and b) AOT solutions, with and without $3.5 \cdot 10^{-3}$ (mono)mol/l PAMPS25 added. 750 ppm correspond to $3.5 \cdot 10^{-3}$ (mono)mol/l. The graph is taken from reference [18].
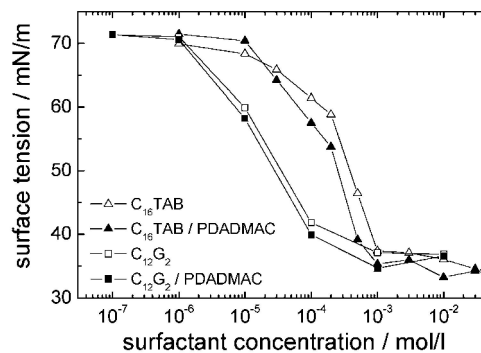

Fig. 8 Dependence of surface tension on the surfactant concentration of the pure surfactant solution (open symbols) and after the addition of $5 \cdot 10^{-3}$ (mono)mol/l PDADMAC and PDADMAC/$C_{12}G_2$. Graph is taken from reference [10]
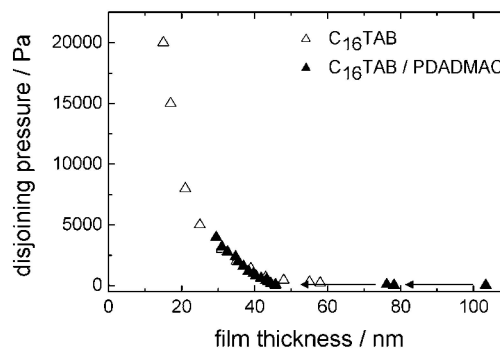

Fig. 9 Disjoining pressure isotherms of a free-standing pure C_{16}TAB film versus a film stabilized by the mixed system C_{16}TAB/PDADMAC. C_{16}TAB: 10^{-2} mol/l and PDADMAC: $5 \cdot 10^{-3}$ (mono)mol/l. The graph is taken from reference [10]

PDADMAC are shown in figure 9. Both pure surfactant and the C_{16}TAB/PDADMAC mixture lead to a CBF and no transition to a NBF was observed. However, after addition of PDADMAC the observed foam films rupture at lower pressure, although the electrostatic repulsion should be stronger due to additional positive charges. It is assumed that the mobility and fluctuation of polyelectrolyte chains might reduce the film stability.

Foam films stabilized by nonionic surfactants at concentrations well below its cmc ($5 \cdot 10^{-5}$ mol/l) form a CBF (figure 10). The electrostatic stabilization is explained by negative charges at the air/water interface resulting from OH$^-$ adsorption[8,39,40]. After the addition of $5 \cdot 10^{-3}$ monoM PDADMAC a CBF to NBF transition is already induced at low pressures at about 800 Pa. In this state the film is only a few nm thick. The NBF is not very stable and ruptures after a few minutes at 800 Pa. A formation of a NBF is also observed for pure $C_{12}G_2$ solutions for high surfactant concentrations[9]. This is explained by the replacement of negative charges at the air/water inter-

face by nonionic surfactants. Another possibility to induce a CBF to NBF transition is the addition of an electrolyte[41]. In both cases the observed NBF is much more stable than the one observed for the PDADMAC-$C_{12}G_2$ mixture. This discrepancy is explained by a higher ordering of the surfactant molecules at the film surface for pure surfactant solutions. In this case the NBF is highly ordered and forms a crystalline thin film[42]. Since PDADMAC does not adsorb at the surface the NBF formation is explained by electrostatic screening of the negative charges at the surface by PDADMAC. Nevertheless, the resulting structure within a NBF seemed to be less ordered. This might be due to a lower packing density of surfactants or the fluctuation of polymer chains which leads to a lower stability of the resulting NBF. In both cases stratification occurs for mixtures of PDADMAC with equally or uncharged surfactants at concentrations studied (see chapter 3).

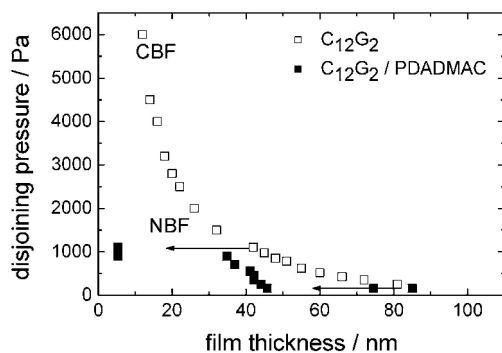To summarize, this example clearly shows that the foam

Fig. 10 Disjoining pressure isotherms of a free-standing pure $C_{12}G_2$ film versus a film stabilized by the mixed system $C_{12}G_2$/PDADMAC. The $C_{12}G_2$ concentration is $5 \cdot 10^{-5}$ mol/l and the PDADMAC concentration $5 \cdot 10^{-3}$ (mono)mol/l. The graph is taken from reference [10]

film stability can be easily tuned by the charge combination of polyelectrolytes and surfactants. It also shows that the type of black film (NBF or CBF) plays a decisive role for the film stability. In contrast to pure surfactant films the NBF is not stable in presence of polyelectrolytes.

2.3 Foam films stabilized by proteins

Proteins are natural polymers consisting of charged hydrophilic segments and neutral hydrophobic segments. In solution, they frequently adopt a compact structure, which can unfold during adsorption at interfaces. If the bulk concentration is high enough, stable foam films can be formed[43].

Foam films formed from partially aggregated proteins are either fluid– or gel–like, depending on the aggregate size and the amount of aggregates[44,45].

Figure 11 shows photos of foam films at a fixed ratio between aggregated and non–aggregated proteins, but for different aggregate sizes. The photos show a clear increase in heterogeneity with increasing aggregate size. In ref.[45] a film phase diagram is presented which accounts the different features of foam films stabilized by β-lactoglobulin solutions with respect to the concentration and size of the protein aggregates. This phase diagram reveals the existence of a critical amount of aggregates above which a gel-like network forms within the film. This amount depends on the aggregate size and concentration of the protein. Below this concentration, foam films are still inhomogeneous but with isolated mobile structures at the film surface. In all cases, gel- like films are more stable than fluid films. The stability of the foam film highly correlates with the stability of the resulting macroscopic foam.

The most simple explanation for the higher stability of gel–

like films is the higher viscosity, which reduces the drainage velocity with respect to fluid films. In addition larger aggregates or networks can block the Plateau borders slowing down the drainage as well. For instance "blocking of Plateau borders" was also used to switch the foam stability by using thermosensitive vesicles, which can change the shape[46,47]. In addition, network-like structure at the surface leads to higher surface elasticity which stabilizes the film due to easier reduction of local fluctuations. In addition, larger protein aggregates at the film surface contribute stronger to electrostatic repulsion and therefore to film stability than small aggregates.

Foam films of sodium caseinate solutions[48] show similar behavior. The inhomogeneities are mobile at low concentration, but they do not longer move when they become interconnected above a certain concentration. Again, this leads to an increased stability of foam films and macroscopic foams.

Maldonado-Valderama et al. investigated foam films composed of the protein casein and a neutral low molecular weight surfactant (Tween 20)[49]. In their study two different types of proteins were investigated. One was the commercial casein (which is a mixture containing different casein proteins), the other one was isolated β-casein (the major component of the commercial casein mixture). Foam films stabilized with the commercial casein are thinner than the ones stabilized with isolated β-casein. The lower film thickness in case of commercial casein correlates with a significantly lower half-lifetime of the respective macroscopic foam. The different behavior of both casein samples is explained by differences in displacement of β-casein by Tween 20. In all cases the thickness and stability for foam films of protein/Tween 20 mixtures were higher than the stability of foam films formed from pure Tween 20 solutions at concentrations above its cmc.

On the other hand pure proteins form brittle monolayers at the air-water interface, that can easily break and leave uncovered area as it is the case for some oppositely charged surfactant-polyelectrolyte mixtures. Surfactants make the rigid protein layer more flexible and mobile, and the layer then might better respond to applied stresses without rupturing[50].

3 Stratification of thin liquid foam films

So far, systems with continuous disjoining pressure isotherms were considered that can be described with the DLVO theory and steric interactions. The effect of the composition of the *film surface* is reflected by the occurrence of a NBF or CBF. Beyond a certain concentration of micelles[51–54], particles[55–58] or polyelectrolytes[9,27,59] oscillatory forces can be measured, which indicates a certain ordering of these mesoscopic objects within the film[60]. Oscillatory forces reflect interactions between mesoscopic objects within the *film bulk* and can be partially separated from interfacial effects. The thin liquid foam films can be considered as a tool to study the effect of geomet-
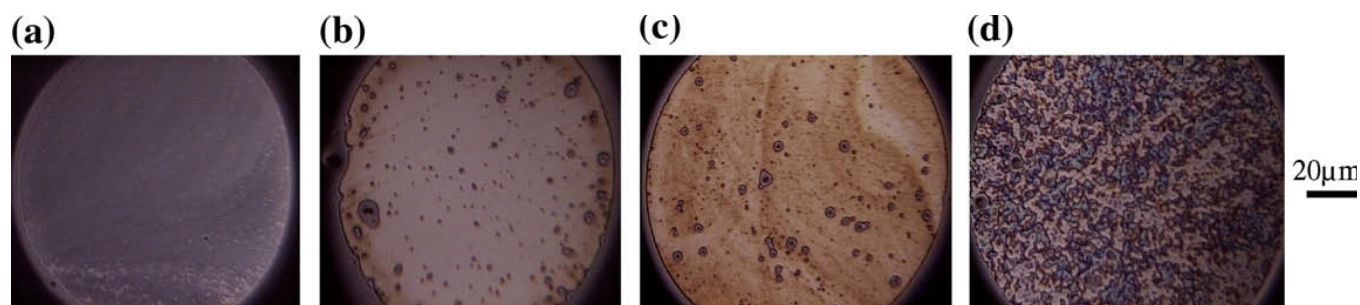
Fig. 11 Top view of foam films stabilized by β-lactoglobulin (bulk concentration 1 g/l) containing 50 % protein aggregates and 50 % non–aggregated proteins. The aggregate size for the respective foam is: a) $R_h = 35 \ nm$ b) $R_h = 71 \ nm$ c) $R_h = 117 \ nm$ d) $R_h = 197 \ nm$. The aggregates were pre–formed at different protein bulk concentrations. (1 g/L, 2 g/L, 8 g/L and 10 g/L). The photo is taken from reference [45].

rical confinement on the ordering of the mesoscopic objects. This phenomenon will be shortly addressed at the end of this chapter. In the following the stratification of foam films as a consequence of oscillatory forces and the effect on the dynamics in foam films containing polyelectrolytes will be discussed.

To investigate stratification behavior in thin liquid films a large number of experiments was performed with polyelectrolyte solutions, often containing small amounts of surfactants for stabilization purposes. The first experiments on thin films made from aqueous polyelectrolyte solutions were performed using AFM and revealed the presence of oscillatory forces, which were attributed to the presence of polymer coils [59] acting similar as surfactant micelles. This interpretation has to be treated carefully as explained in section 3.1 below.

The first TFPB experiments on foam films containing polyelectrolytes evidenced similar oscillations [18]. For disjoining pressure isotherms of foam films stabilized with C_{12}TAB/PAMPS jumps in film thickness ($\Delta(h)$) were observed when increasing the applied pressure.
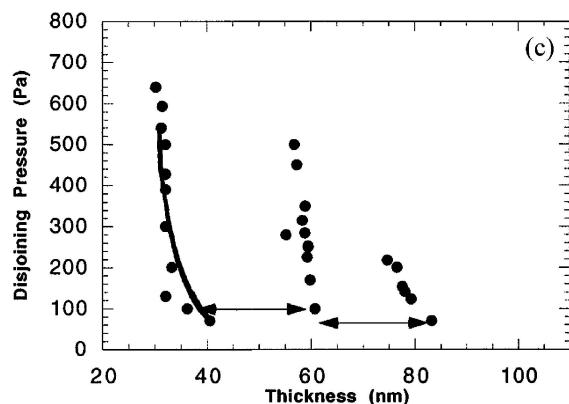

Fig. 12 Stepwise thinning for a foam film stabilized by a mixture of $5 \cdot 10^{-5}$ mol/lC_{12}TAB and $8.6 \cdot 10^{-3}$ (mono)mol/l PAMPS25. The graph is taken from reference [27].

The jump in film thickness is attributed to the transition between two neighbored branches of a disjoining pressure isotherm as shown in figure 12. The transition is observed by the appearance of darker domains, corresponding to the new thinner film thickness. The domains expand over the whole film and form the new thinner film. This stratification is not reversible. If the pressure is decreased the film stays on the same branch of the isotherm and the film thickness does not increase much.

The occurrence of oscillatory forces is explained by expulsion of quantized amounts of polymer chains as explained below.

3.1 Effect of the polymer system

Stratification is easily observed for films containing rather flexible polyelectrolytes, *i.e.* polymers with a relatively low persistence length like PAMPS, PSS and carboxymethyl-chitin (CM-Chitin). If at all, stratification is much more difficult to observe for stiff polyelectrolytes like DNA and Xanthane [61]. It is assumed that the time scale for polymer network relaxation increases with increasing backbone rigidity. Stratification with stiffer polymers is only observed when the viscosity is large enough so that the polymer network has time to adjust and remain in equilibrium while thinning is taking place. Similarly, stratification is only seen with films confined between solid surfaces when the velocity of approach is slow enough. This was realized with a CP–AFM which allows adjusting the velocity of approach of the opposing surfaces [61].

The jump size Δh of the oscillation period depends on the properties of the polymer like chemical structure, charge density and concentration. In general the stepwise thinning of the foam film is observed in the semi-dilute concentration regime above c* of the polyelectrolyte but below the cac [18]. Stratification occurs due to the oscillation of the disjoining pressure in the film and is assumed to originate in a transient polyelectrolyte network that is formed in the film core above the overlap concentration of the polymer c* [28,35,62,63]. It was shown

first by Asnascios et al.[27] that the oscillation period decreases as the square root of the polymer concentration (figure 13) and is independent of molecular weight[36].
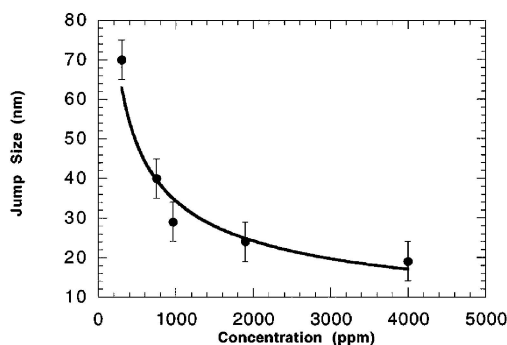

Fig. 13 Distances d between the branches of the disjoining pressure curves versus polymer concentration. The graph is taken from reference[27].

Depending on the geometry of the polymer backbone the observed step size either scales with Δh proportional $c^{-1/2}$ for linear polyelectrolytes and Δh proportional $c^{-1/3}$ for branched polyelectrolytes[37,64]. Branched polymers can be considered as charged spheres and show the typical scaling law of objects, ordered in 3 dimensions[58]. In the case of linear polyelectrolytes the scaling law $\Delta h \propto c^{-1/2}$ reflects the formation of a polyelectrolyte network with a mesh size ξ. The mesh size of the respective bulk solution was determined by small angle neutron or x-ray scattering (SANS, SAXS). It was shown that the distance between the polyelectrolyte chains ($\xi = 2\pi/q_{max}$) obtained from the position q_{max} of the structure peak is equal to the jump size Δh of the film stratification[36]. This means that there is no effect of geometrical confinement on the average distance of polyelectrolyte chains (*i.e.* mesh size) within the network. The similarity between jump size in the film and network mesh size in the bulk is explained by the fact that the network is transient (breaks down and rebuilds) and fits into the available volume. If the film thickness becomes too small due to increase of the outer pressure for n meshes the network rebuilds with $n-1$ meshes. The relation between the film stratification and the pair correlation function is explained in section 3.4.

The stratification is affected by the ionic strength. With increasing ionic strength, the number of visible oscillations and their amplitude decreases, until they disappear at high salt concentrations (around 10^{-2} mol/l)[27,65]. This is well correlated with SANS experiments, where a characteristic peak disappears above 10^{-2} mol/l salt[36].

The degree of polymer charge has also a strong impact on the stratification behavior. With decreasing charge density the amplitude of oscillatory forces decreases[65]. For highly

charged polymers the disjoining pressure isotherm is divided into several pronounced branches and multiple stratification occurs stepwise at successive higher pressure (empty squares in figure 14. On contrary, in films stabilized with polyelectrolytes with a low degree of charge all steps take place simultaneously at very low disjoining pressures (● and photo in figure 14).
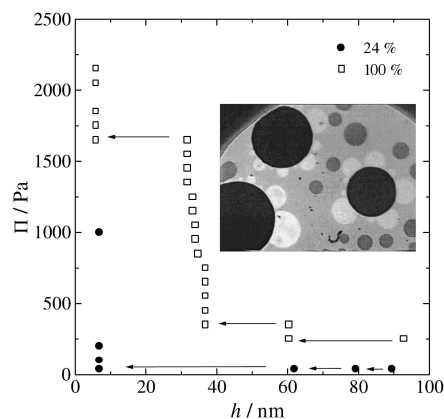

Fig. 14 Disjoining pressure as a function of film thickness for APG/PDADMAC films at two different degrees of PDADMAC charge: 100% (fully charged chain) and 24%. The graph is taken from[9]. The photo is taken from reference[65].

3.2 Effect of surfactant

In general, stratification phenomena are not affected by the choice of surfactant with respect to the step size[33,38]. Figure 15 displays disjoining pressure isotherms for solutions containing $3.8 \cdot 10^{-3}$ (mono)mol/l carboxyMC and 10^{-4} mol/l surfactant varying in chain length from 12 to 16 carbon atoms. Stratification was observed for all C_nTAB systems, and the size of the thickness jump is almost the same (23–25 nm). The only difference is that foam films stabilized from C_{12}TAB mixtures are less stable than those with C_{14} or C_{16}TAB. Also the influence of different surfactant types was investigated. The same step size was observed for a mixture of $3.8 \cdot 10^{-3}$ (mono)mol/l carboxyMC with the anionic surfactant AOT. Similar observations were made for the anionic PSS using either the cationic C_{12}TAB or a neutral surfactant[28] and mixtures of the cationic PDADMAC and either C_{16}TAB or $C_{12}G_2$ [38] (compare figure 9 and figure 10). CP–AFM experiments on solutions containing polyelectrolytes with and without surfactants confirmed that the choice of surfactant does not influence the occurrence and the step–size of stratification[61]. This is a strong hint, that the stratification is a confinement phenomenon and that the properties of the film surfaces play a minor role. This point is addressed more in detail in section 3.4.
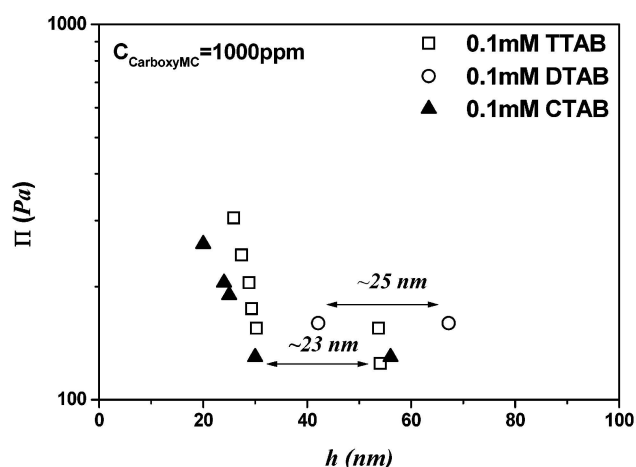
Fig. 15 Disjoining pressure versus film thickness for mixed solutions of 10^{-4} mol/l C_nTAB and $3.8 \cdot 10^{-3}$ (mono)mol/l carboxyMC. The graph is taken from reference [33].

Although the surfactant has no effect on the step size, it influences strongly the kinetics of stratification as shown in the following section.

3.3 Kinetics of stratification

According to the Navier Stokes equation (creeping flow limit) the drainage velocity of liquid films is proportional to the inverse viscosity of the respective bulk solution. This principal relation was also found for the effective diffusion coefficient D of the rim during wetting of stratified drops ($D \propto 1/\eta_{eff}$ [66,67]), but the viscosity of a thin film (η_{eff}) can differ from the bulk viscosity of the respective bulk solution (η). The stratification of a foam film is also considered as a dewetting phenomenon and the effective diffusion coefficient is [68]

$$ D = -\frac{h_\infty^3}{12\eta_{eff}} \frac{\partial \Pi}{\partial h} \qquad (1) $$

where h_∞ is the equilibrium film thickness far from the opening domain. The opening velocity, related to the change in area with time is directly measured by video microscopy

$$ D' = \frac{\partial r^2}{\partial t} \qquad (2) $$

and has the dimension of a diffusion coefficient. The relationship between D' and D is described by [69], and D' is only a few percent of D [70].

There is a strong effect of the polyelectrolyte and surfactant charge on the stratification kinetics. One has to distinguish the polymer adsorbing and polymer non–adsorbing case. Furthermore it is important if one considers the opening velocity

or the effective viscosity η_{eff} [70]. According to eq. 1 η_{eff} takes the disjoining pressure gradient $\frac{\partial \Pi}{\partial h}$ of each branch during stratification into account.

1) *Opening velocity of domains:* In case of oppositely charged surfactants and polyelectrolytes complexes are formed at the film interface. With decreasing film thickness the opening velocity decreases. The transition from a film containing 3 layers of polyelectrolyte network to a 2–layer film is faster than for a $2 \rightarrow 1$ layer transition. This was found for $C_{12}TAB$/PAMPS and $C_{12}TAB$/CMC films [69,70]. One reason for the decrease in velocity might be dangling polyelectrolyte chain at the film interface. In case of non-adsorbing polyelectrolytes the opening velocity is much faster: factor 3 for the non-ionic surfactant $C_{12}G_2$ [70] and factor 6 for the equally charged surfactant AOT [71]. The higher velocity for AOT can be explained by a strong electrostatic repulsion. The repulsion might also lead to an increasing velocity of stratification with decreasing film thickness. In contrast to oppositely charged surfactants and polyelectrolytes, now the transition from a film containing 2 layers of polyelectrolyte network to a 1–layer film is faster than for a $3 \rightarrow 2$ layer transition [71] (see 0.3 wt–% in figure 16a).

More difficult to understand is the effect of the polyelectrolyte concentration on the opening velocity of the domains. Oppositely charged surfactants and polyelectrolytes and mixtures with non–ionic surfactants show a decrease in opening velocity with increasing polyelectrolyte concentration [70]. In contrast, no systematic effect of polyelectrolyte concentration on the opening velocity was detected for equally charged surfactants and polyelectrolytes [71] (see figure 16a). There, only the film thickness seems to be decisive for the opening velocity. So far, an explanation for the difference is still missing. The bulk viscosity does not change significantly within the studied polyelectrolyte concentration regime. Therefore, the change in surface properties might be a reason, i.e. η_{eff} increases. With increasing polyelectrolyte concentration the tendency for polyelectrolyte adsorption increases, mediated by surfactants. This decreases the drainage velocity as mentioned above for thin foam films. In case of equally charged polyelectrolytes and surfactants the polyelectrolyte adsorption is prevented due to electrostatic repulsion.

2) *Effective viscosity:* Considering the effective viscosity the differences in stratification between oppositely charged surfactant and polyelectrolyte and mixtures with non–ionic surfactants vanish [70]. Interestingly, the ratio η_{eff}/η increases with increasing polyelectrolyte concentration (see figure 16b). If there were just bulk effects due to increasing polyelectrolyte concentration η_{eff}/η should be constant in figure 16b. The increase is a strong hint for increasing dissipation with increasing polyelectrolyte concentration. In addition, figure 16b shows for oppositely charged surfactants and polyelectrolytes that η_{eff}/η increases with decreasing film thickness ($3 \rightarrow 2$

movement of the domain border shows diffusion–like behavior ($r(t) \propto t^{1/2}$). This is a typical feature of domains with a smooth rim without any Rayleigh instabilities[72]. The layer of mixed $C_n TAB$/carboxyMC complexes at the film surfaces is assumed to slow down the opening of the stratification domains. In contrast, in presence of the anionic surfactant AOT no complex layer with the equally charged carboxyMC is formed at the film surface. This leads to a faster transition and thicker droplets (Rayleigh instabilities) are formed at the domain border. The domain border moves with constant velocity ($r(t) \propto t$)[33]. In further studies for AOT/CarboxyMC a
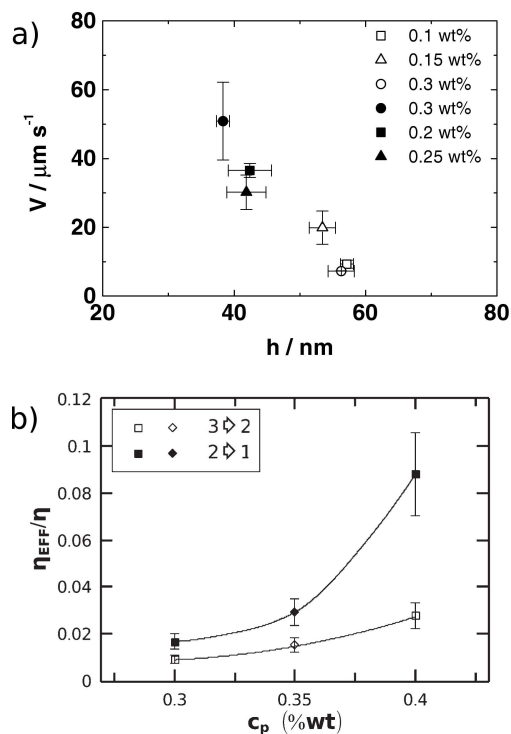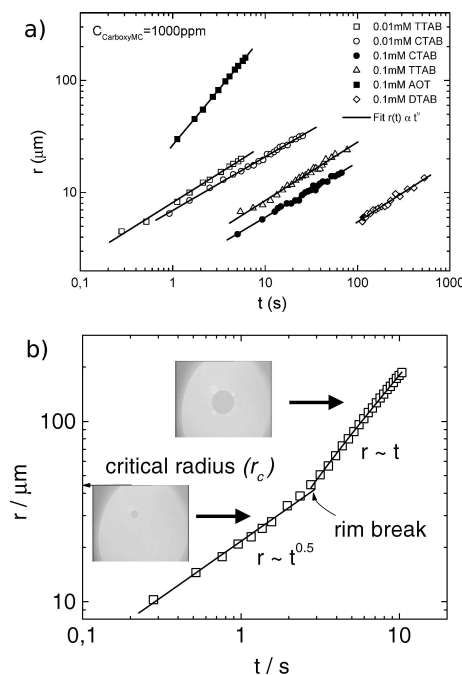

Fig. 16 a) AOT/carboxyMC foam film during stratification: opening velocity of the domains as a function of the film thickness for different carboxyMC concentrations at 0.1 mM AOT. At 0.3 wt–% 2 transitions occur, all other carboxyMC concentrations give one transition. The graph is taken from reference[71]. b) PAMPS/C_{12}TAB foam film during stratification: film viscosity (η_{eff}) normalized by the viscosity (η) of the respective bulk solution in dependence of PAMPS concentration for two different transitions. The graph is taken from reference[70].

Fig. 17 a) Time dependence of the stratification domain radius r(t) for AOT/ CarbocyMC and C_nTAB/CarboxyMC systems. The solid lines correspond to fits with r(t)~ t for AOT and r(t)~ $t^{1/2}$ for C_nTAB. The concentration of 1000 ppm (0.1 wt%) corresponds to $3.8 \cdot 10^{-3}$ (mono) mol/l carboxyMC (DS = 1.23). The graph is taken from reference[33]. b) Typical time dependence of the radius of domains for carboxyMC concentration of 0.15 wt% (1500 ppm = $5.7 \cdot 10^{-3}$ (mono)mol/l). The graph is taken from reference[71].

vs. 2 → 1 layers transition) which is a strong hint for increasing dissipation with decreasing film thickness. The increase in η_{eff}/η leads to the decrease in opening velocity as mentioned above. Unfortunately, there is no graph like figure 16b for the system AOT/carboxyMC in literature. According to the considerations made above, one would expect that η_{eff}/η AOT/carboxyMC remains constant irrespective of the concentration and that η_{eff}/η decreases with decreasing film thickness.

In case of foam films the choice of surfactant/polyelectrolyte composition has an effect on the characteristic time behavior for the different systems and a strong relation to Rayleigh instabilities.

Figure 17 shows that the kinetics of liquid films containing a polyanion (carboxyMC) are very sensitive to the nature of the surfactant. When cationic surfactants (C_nTAB) are added to carboxyMC, a slower stratification is found and the

transition from a diffusion–like stratification kinetic to a linear one was found at a specific domain radius r_c[71]. The transition was accompanied by the occurrence of rim instabilities (Rayleigh instabilities).

To summarize, foam films with a *faster* transition kinetics (*equally* charged surfactant and polyelectrolyte) show a transition from $r(t) \propto t^{1/2}$ to $r(t) \propto t$ accompanied by Raleigh instabilities while more *slowly* expanding domains (*oppositely* charged surfactant and polyelectrolyte) grow always as $r(t) \propto t^{1/2}$.

What do the exponents $r(t) \propto t^{1/2}$ and $r(t) \propto t$ mean in terms of slip/no slip conditions? In case of no-slip conditions one would expect a constant velocity ($r \propto t$) and for slip conditions $r \propto t^{2/3}$ [73,74]. An increase of the domain radius r with $t^{1/2}$ was found for stratification of foam films containing micelles [75] or for stratified polymer films [76]. The exponent 1/2 as also found for foam films with oppositely charged is closer to the exponent 2/3 for slip conditions. However, it is not very likely that a water layer can slip on another water layer. Heinig [69] extended a model, which was originally used for the opposite phenomenon: spreading of microcopic droplets [68]. In the model the domain expansion is assumed to be driven by capillary forces. The model uses lubrication approximation with no-slip boundary conditions at the surface of the film and is summarized in ref. [70].

The trends exhibited by the stratification kinetic are opposite to the trends found for film stability: AOT/CarboxyMC films are more stable than C_nTAB/CarboxyMC as mentioned in capter 2, but their transition kinetics is faster. For continuously draining films a reduction in drainage velocity e.g. by increase in viscosity can increase the film stability [2]. An explanation for the counter intuitive behavior during stratification might be the strong electrostatic repulsion between AOT and CarboxyMC that accelerates the expulsion of polyelectrolyte chains from the bulk but also stabilizes the film.

3.4 Comparison with oscillatory forces through polyelectrolyte solutions confined between two solid surfaces

Due to the fact that a CP–AFM allows measuring more or less the complete oscillation, CP–AFM is a more versatile tool to characterize the oscillatory forces [58]. In addition this method allows adjusting the approach velocity of the two opposing surfaces which is of interest for kinetic studies [61,70].

In the experiments described in the following the forces were measured between the colloidal Silica microsphere and a planar Silicon wafer. The force curves are characterized by three parameters: the period of the oscillation (ξ), the exponential envelope (decay length) λ and the amplitude. These parameters are compared quantitatively with the measurable sizes obtained from scattering experiments at the respective bulk solutions as followed: The period of the force curves is compared to the inverse position of the structure peak ($2\pi/q_{max}$) and indicates the mesh size of the polyelectrolyte network. The decay length of the force curve is compared to the inverse width of the structure peak ($1/\Delta q$) and is attributed to the range of ordering. The amplitudes of both methods indicate the strength of ordering but can only be qualitatively compared. The effect of outer and inner parameters like ionic strength, polyelectrolyte charge density and molecular weight are the same as for foam films.

It is worth noticing that there are some differences with respect to the TFPB measurements:
1) A CP–AFM allows measuring oscillatory forces in both the dilute regime (interchain distance $\propto c^{-1/3}$, polyelectrolyte coils) and the semi–dilute regime (interchain distance $\propto c^{-1/2}$, polyelectrolyte network), while with the TFPB oscillatory forces are only accessible in the semi–dilute regime.
2) In CP–AFM experiments a slight compression of the chains by a maximum 20% and an increase of counterion condensation at the PSS chains could be detected due to confinement.
3) Due to the fact that with the CP–AFM the full oscillation is acessible, the decay length can be measured. The decay length is larger than the Debye length [77,78]. It gives the same value as the range of ordering in the bulk solution.

Thereby it is unclear if the reason for the difference is the higher precision of the CP–AFM or the fact that the measurements are carried out between two solid interfaces instead of to fluid interfaces. For Silica dispersions confined in a CP–AFM it has been shown that the structural forces (which corresponds to stratification in foam films) are an effect of confinement. The oscillation period is very robust against changes in elasticity of the surface (fluid or solid) [79], surface charge [80], surface roughness [81], ionic strength [82] and against (non)presence of surfactants of different charges [79]. On the other hand, these parameters affect the amplitude (strength of ordering) and the decay length (range of ordering).

In general it is worth noticing that the oscillatory curve that is measured by a CP–AFM correspond to the pair correlation function of the polyelectrolyte solution and presents the inverse Fourier transform of the structure factor of the solution measured by SANS or SAXS. The branches measured by TFPB correspond to the repulsive parts of the pair correlation function.

4 Conclusion and open questions

The results presented in the review lead to the conclusion that the film can be divided into the two *interfacial regions* with an excess of surfactant and the *film core* containing a geometrically confined polyelectrolyte solution. Repulsion of the polyelectrolyte chains within the film core from the film surface leads to stable foam films. This is the case for *a*) equally charged and *b*) oppositely charged polyelectrolytes and surfactants and *c*) for the combination of polyanions and non–ionic surfactants. In case of oppositely charged compounds (case *b*) this simple consideration is only valid below the cac. Above the cac polyelectrolyte/surfactant bulk aggregates are formed which block the drainage and lead to ultrastable films. For case *c* one has to take into account that the air/water interface is assumed to be negatively charged and only polyanions are repelled. In contrast, in foam films of polycations and non–ionic surfactants, polycations are attracted by a film

surface, which leads to less stable foam films.

Replacing the synthetic polymers by proteins shows that not only the adsorbed amount but also the lateral structuring of proteins affects the stability. The formation of percolated networks of particles leads to higher stabilisation. This has been recently found also for nanoparticles in Pickering foams [83], and proteins can be also considered as particles.

In contrast to pure surfactant foam films mixed polyelectrolyte/surfactant foam films show a lower stability in concentration regimes around the isoelectric point (IEP) going with high elasticity and low surface tension. This indicates that the electrostatic repulsion between both surfaces determines the film stability. The electrostatic repulsion is reduced if a lot of material is adsorbed due to charge compensation of polyelectrolyte and surfactant.

The minimum in foam film stability with increasing polyelectrolyte implies a continuously increasing amount of adsorbed polyelectrolyte leading to a charge reversal close to the IEP. Results of surface tension and surface elasticity measurements do not support this simple image. Close to the IEP the surface tension shows a minimum and the elasticity a maximum which indicates a maximum in adsorbed amount. So far, it is not clear, why the adsorption maximum occurs at at low polyelectrolyte concentrations and low surfactant concentrations. A speculation is the formation of two different types of aggregates: one around the IEP with flat adsorbed polyelectrolyte chains and one type at higher polyelectrolyte concentrations with long tails dangling into the solution.

Above the overlap concentration c* the polyelectrolyte chains overlap in the bulk solution and a transient network is formed. This leads to oscillatory forces under confinement in a thin film. The comparison with results of SAXS and SANS measurements show that the characteristic parameters like mesh size of the network and range of ordering do not change during confinement. The mesh size scales with $c^{-1/2}$ for linear polyelectrolytes and with $c^{-1/3}$ for branched polyelectrolytes and is very robust against changes in properties of the outer surfaces (charge, elasticity, roughness). This indicates that the oscillatory forces present properties of the film core independent of the properties of the confining surfaces. A decrease in polyelectrolyte charge or an increase in ionic strength leads to a decrease in amplitude of the oscillatory forces.

While the surface properties have no effect on the structuring of the polyelectrolytes under confinement they have a strong impact on the transition kinetics of the during film stratification. In case of equally charged polyelectrolytes and surfactant the kinetics is quite fast due to strong electrostatic repulsion across the foam film and due to smooth interfaces. The effective viscosity decreases with decreasing film thickness. In case of oppositely charged polyelectrolytes and sur-

factants the film surface is rather rough due to dangling ends directed towards the film core. This slows down the expulsion of polyelectrolytes and increases the effective viscosity with decreasing film thickness.

The absolute values for η_{eff} are controversially discussed in literature. Both, values more than an order of magnitude higher [69] and lower [70] than the bulk viscosity are reported. Another weak point is that neither the Marangoni effect nor surface rheology is included within the model. All these effects are combined in the effective viscosity η_{eff}, which does not allow to split up the different contributions.

Acknowledgement

References

1 P. Hansson and B. Lindman, *Current Opinion in Colloid & Interface Science*, 1996, **1**, 604–613.

2 I. Ivanov and D. Dimitrov, *Thin Liquid Films, p. 379*, Marcel Dekker, New York, 1988.

3 D. Exerova and P. M. Kruglykov, *Foam and Foam Films Theory, Experiment, Application*, Elsevier, Amsterdam, 1998.

4 K. J. Mysels and M. N. Jones, *Discuss Faraday Soc.*, 1966, **42**, 42–50.

5 D. Exerowa and A. Scheludko, *Chim. Phys. Bulgarien*, 1971, **24**, 47.

6 D. Exerowa, T. Kolarov and K. H. R. Khristov, *Colloids Surfaces*, 1987, **22**, 161–169.

7 R. von Klitzing, *Adv. Colloid Interface Sci.*, 2005, **114**, 253–266.

8 K. Ciunel, M. Armelin, G. H. Findenegg and R. von Klitzing, *Langmuir*, 2005, **21**, 4790–4793.

9 C. Stubenrauch and R. von Klitzing, *J. Phys. Condens. Matter*, 2003, **15**, R1197–R1232.

10 N. Kristen and R. von Klitzing, *Soft Matter*, 2010, **6**, 849.

11 W. Ducker, T. Senden and R. Pashley, *Nature*, 1991, **353**, 239.

12 A. Asnacios, D. Langevin and J. F. Argillier, *Macromolecules*, 1996, **29**, 7412–7417.

13 A. Asnacios, R. von Klitzing, R.Klitzing and D. Langevin, *Colloids Surf. A*, 2000, **167**, 189–197.

14 C. Stubenrauch, P. A. Albouy, R. von Klitzing and D. Langevin, *Langmuir*, 2000, **16**, 3206–3213.

15 D. J. F. Taylor, R. K. Thomas and J. Penfold, *Langmuir*, 2002, **18**, 4748–4757.

16 N. Kristen, A. Vüllings, A. Laschewsky, R. Miller and R. von Klitzing, *Langmuir*, 2010, **26**, 9321–7.

17 N. Kristen-Hochrein, R. Miller and R. von Klitzing, *Journal of Physical Chemistry B*, 2011, **115**, 14475 – 14483.

18 V. Bergeron, D. Langevin and A. Asnacios, *Langmuir*, 1996, **12**, 1550–1556.

19 *Interactions of Surfactants with Polymers and Proteins*, ed. E. Goddard and K. Ananthapadmanabhan, CRC Press, 1993.

20 C. Monteux, C. E. Williams and V. Bergeron, *Langmuir*, 2004, **20**, 5367–5374.

21 S. Guillot, M. Delsanti, S. Desert and L. D., *Langmuir*, 2003, **19**, 230–237.

22 S. Trabelsi and D. Langevin, *Langmuir*, 2007, **23**, 1248–1252.

23 S. Trabelsi, E. Raspaud and D. Langevin, *Langmuir*, 2007, **23**, 10053–10062.

24 G. Espinosa and D. Langevin, *Langmuir*, 2009, **25**, 12201–7.

25 C. Bain, P. Claesson, L. D., R. Meszaros, T. Nylander, C. Stubenrauch and R. Titmuss, S.and von Klitzing, *Advances in Colloid and Interface Science*, 2010, **155**, 32?49.

26 E. Carey and C. Stubenrauch, *Journal of Colloid and Interface Science*, 2010, **343**, 314–23.

27 A. Asnacios, A. Espert, A. Colin and D. Langevin, *Phys. Rev. Lett.*, 1997, **78**, 4974–4977.

28 R. von Klitzing, A. Espert, A. Asnacios, T. Hellweg, A. Colin and D. Langevin, *Colloids Surfaces A*, 1999, **149**, 131–140.

29 V. Bergeron, *Langmuir*, 1997, **13**, 3474–3482.

30 L. Bergstrm, *Advances in Colloid and Interface Science*, 1997, **70**, 125–169.

31 C. Stubenrauch, F. B., E. Aksenenko and R. Miller, *J. Phys. Chem. B*, 2005, **109**, 1505–1509.

32 N. Kristen, V. Simulescu, A. Vllings, A. Laschewsky, R. Miller and R. v. Klitzing, *J. Phys. Chem. C*, 2009, **133**, 7986–7990.

33 C. Beltran, S. Guillot and D. Langevin, *Macromolecules*, 2003, **36**, 8506–8512.

34 O. Theodoly, J. S. Tan, R. Ober, C. E. Williams and V. Bergeron, *Langmuir*, 2001, **17**, 4910–4918.

35 J. L. Toca-Herrera and R. von Klitzing, *Macromolecules*, 2002, **35**, 2861–2864.

36 R. von Klitzing, B. Kolaric, W. Jaeger and A. Brandt, *Phys. Chem. Chem. Phys.*, 2002, **4**, 1907–1914.

37 R. von Klitzing and B. Kolaric, *Prog. Colloid Polym Sci*, 2003, **122**, 122,9.

38 B. Kolaric, W. Jaeger, G. Hedicke and R. von Klitzing, *J. Phys. Chem. B*, 2003, **107**, 8152–8157.

39 C. Stubenrauch, J. Schlarmann and R. Strey, *Phys. Chem. Chem. Phys.*, 2002, **4**, 4504–4513.

40 N. Schelero and R. von Klitzing, *Soft Matter*, 2011, **7**, 2936–2942.

41 V. Bergeron, A. Waltermo and P. Claesson, *Langmuir*, 1996, **12**, 1336.

42 L. Evers, E. Nijman and G. Frens, *Coll. Surf. A*, 1999, **149**, 521–527.

43 T. Dimitrova, F. Leal-Calderon, T. Gurkov and B. Campbell, *Langmuir*, 2001, **17**, 8069–8077.

44 B. Rullier, M. Axelos, D. Langevin and B. Novales, *Journal of Colloid and Interface Science*, 2009, **336**, 750–752.

45 B. Rullier, M. Axelos, D. Langevin and B. Novales, *Journal of Colloid and Interface Science*, 2010, **343**, 330–337.

46 A. L. Fameau, A. Saint-Jalmes, F. Cousin, B. H. Houssou, B. Novales, L. Navailles, F. Nallet, C. Gaillard, F. Boue and J.-P. Douliez, *Angew. Chem. Int. Ed.*, 2011, **50**, 8264.

47 A. Carl and R. von Klitzing, *Angew. Chem. Int. Ed.Inter. Ed.*, 2011, **50**, 11290–11292.

48 A. Saint-Jalmes, M.-L. Peugeot, H. Ferraz and D. Langevin, *Colloids and Surfaces A*, 2005, **263**, 219–225.

49 J. Maldonado-Valderrama and D. Langevin, *Journal of Physical Chemistry B*, 2008, **112**, 3989–3996.

50 M. Bos and T. van Vliet, *Advances in colloid and interface science*, 2001, **91**, 437–71.

51 A. Nikolov and D. Wasan, *J. Colloid and Interface Science*, 1989, **133**, 1.

52 A. Nikolov, D. Wasan, N. Denkov, P. Kralchevsky and I. Ivanov, *Prog. Colloid Polym. Sci.*, 1990, **82**, 87.

53 V. Bergeron and C. Radke, *Langmuir*, 1992, **8**, 3020.

54 A. Sonin and D. Langevin, *Europhys. Lett.*, 1993, **22**, 271.

55 E. Perez, J. Proust and L. Ter-Minassian-Saraga, *Thin Liquid films, p. 891*, Marcel Dekker, 1988.

56 E. Basheva, A. Nikolov, P. Kralchevsky, I. Ivanov and D. Wasan, *Surfactants in Solution, vol. 11*, Plenum Press New York, 1991.

57 A. Nikolov and D. Wasan, *Langmuir*, 1992, **8**, 2985.

58 S. Klapp, Y. Zeng, D. Qu and R. von Klitzing, *Phys. Rev. Lett.*, 2008, **100**, 118303.

59 A. Milling, *J. Phys. Chem.*, 1996, **100**, 8986.

60 R. von Klitzing, E. Thormann, T. Nylander, D. Langevin and S. C., *Adv. Colloid Interface Sci.*, 2010, **155**, 1931.

61 F. Kleinschmidt, C. Stubenrauch, J. Deacotte, R. v. Klitzing and D. Langevin, *J. Phys. Chem. B*, 2009, **113**, 3972–3980.

62 R. von Klitzing, A. Espert, A. Colin and D. Langevin, *Colloids Surfaces A*, 2001, **176**, 109–116.

63 R. von Klitzing and H. Mueller, *Curr Opin Coll Interf Sci*, 2002, **7**, 18.

64 R. von Klitzing and B. Kolaric, *Tenside Surfactants Detergents*, 2002, **39**, 247–253.

65 B. Kolaric, W. Jaeger and R. von Klitzing, *J. Phys. Chem. B*, 2000, **104**, 5096–5101.

66 P. de Gennes, *C.R. Acad. Sci. Paris*, 1984, **298**, 475.

67 P. de Gennes and A. Cazabat, *C.R. Acad. Sci. Paris*, 1990, **310**, 1601.

68 J. F. Joanny and P.-G. de Gennes, *C. R. Acad. Sci.*, 1984, **299**, 279–283.

69 P. Heinig, C. Beltran and D. Langevin, *Phys. Rev. E*, 2006, **73**, 051607.

70 J. Delacotte, E. Rio, F. Restagno, C. Uzüm, R. von Klitzing and D. Langevin, *Langmuir*, 2010, **26**, 7819–23.

71 C. Beltran and D. Langevin, *Phys. Rev. Lett.*, 2005, **94**, 217803.

72 A. Sonin, A. Bonfillon and D. Langevin, *Phys. Rev. Lett.*, 1993, **71**, 2342–2345.

73 C. Redon, J. B. Brzoska and F. Brochard-Wyart, *Macromolecules*, 1994, **27**, 468–471.

74 G. Reiter and R. Khanna, *Langmuir*, 2000, **16**, 6351.

75 P. Kralchevsky, A. Nikolov, D. Wasan and I. Ivanov, *Langmuir*, 1990, **6**, 1180.

76 M. P. Valignat, G. Oshanin, S. Villette, A. M. Cazabat and M. Moreau, *Phys. Rev. Lett.*, 1998, **80**, 5377–5380.

77 D. Qu, J. S. Pedersen, S. Garnier, A. Laschewsky, H. Moehwald and R. v. Klitzing, *Macromolecules*, 2006, **39**, 7364–7371.

78 C. Üzüm, S. Christau and R. von Klitzing, *Macromolecules*, 2011, **44**, 7782–7791.

79 Y. Zeng and R. von Klitzing, *Soft Matter*, 2011, **7**, 5329.

80 S. Grandner, R. Zeng, von Klitzing and S. Klapp, *Jounal of Chemical Physics*, 2009, **131**, 154702.

81 Y. Zeng and R. von Klitzing, *Langmuir*, 2012, **28**, 6313–6321.

82 S. Klapp, S. Grandner, Y. Zeng and R. von Klitzing, *Soft Matter*, 2010, **6**, 2330–2336.

83 A. Carl and R. von Klitzing, *submitted*, 2014.